

Cluster structure and hydrogen in Ti–Zr–Ni quasicrystals and approximants

E.H. Majzoub^{a,*}, J.Y. Kim^a, R.G. Hennig^a, K.F. Kelton^a, P.C. Gibbons^a, W.B. Yelon^b

^a Department of Physics, Washington University, St. Louis, MO 63130, USA

^b Research Reactor, University of Missouri, Columbia, MO 65211, USA

Received 30 August 1999; accepted 2 November 1999

Abstract

Elastic neutron diffraction data from icosahedral $\text{Ti}_{45}\text{Zr}_{38}\text{Ni}_{17}$ are presented and analyzed using information from the 1/1 approximant $\text{Ti}_{50}\text{Zr}_{35}\text{Ni}_{15}$. These data indicate that similar clusters exist in the approximant and the i-phase. This is shown to be consistent with simulated diffraction from an icosahedral glass model of the quasicrystal, placing a Bergman cluster on the glass sites. An electrochemical method was used to hydrogenate Ti-based quasicrystals and their crystal approximants. This technique gives a consistently high hydrogen to metal atom ratio of 1.9, without crystal hydride formation in the quasicrystal. © 2000 Elsevier Science B.V. All rights reserved.

Keywords: Icosahedral quasicrystal; Icosahedral glass; Electrolytic hydrogen loading; Ti–Zr–Ni; Bergman cluster

1. Introduction

The atomic structure of quasicrystals is still an open question. Much effort has been spent in investigating the structure of the Al-based quasicrystals. We have considered the Ti–Zr–Ni system, which offers the possibility of using hydrogen as a probe for the local atomic structure. In this paper we present and discuss a model for the structure of the quasicrystal as well as a method for loading hydrogen into the quasicrystal without the production of crystal hydrides.

2. Experimental methods

Alloy ingots of the desired composition for the rapidly quenched quasicrystal, $\text{Ti}_{45}\text{Zr}_{38}\text{Ni}_{17}$, and its annealed 1/1 approximant, $\text{Ti}_{50}\text{Zr}_{35}\text{Ni}_{15}$, were made by arc-melting mixtures of 99.9% purity elements on a water-cooled Cu hearth in a high-purity Ar gas atmosphere. Ribbons of the icosahedral quasicrystal were produced from the alloy ingots by rapid quenching from a graphite crucible onto a rotating Cu wheel. Details of the quenching process can be found elsewhere [1]. The 1/1 ingots were placed in a graphite crucible, which was in turn placed in a quartz tube with a Ti–Zr alloy ingot, to be used as an oxygen getter. The tube was then evacuated to 10^{-2} – 10^{-1} Pa, backfilled with Ar to 1.6×10^4 Pa,

and sealed. To prevent oxygen contamination during annealing, the Ti–Zr getter was first heated to 1000°C for 10 min by rf-induction, while keeping the alloy ingot in the graphite crucible at room temperature. The tube containing the sample and the getter was then annealed in a furnace for 6 days at 600°C to obtain the 1/1 phase.

Samples were characterized by transmission electron microscopy (TEM) and X-ray diffraction for quality and phase purity of the quasicrystal, using a Rigaku powder diffractometer with Cu $K\alpha$ radiation and a JEOL 2000FX TEM. Before hydrogenation the quenched ribbons were powdered by grinding under ethanol. The powder was then dried and pressed into a 1.3 cm diameter pellet weighing between 0.1 and 0.5 g using a pressure $\geq (6.0 \pm 0.7) \times 10^8$ Pa. Samples to be used for open cell potential measurements were pressed with Ni powder (–120 mesh) at a ratio of Ni to sample of approximately 4:1.

Two electrochemical cells were used, one for simply loading the materials with hydrogen, the other for a controlled loading where open cell potential measurements could be performed. Both cells consisted of a Pyrex dish containing 100–150 ml of 6 M KOH solution. Samples were suspended by electrical connectors that did not enter the solution, causing a portion of the sample to protrude above the electrolyte bath. The counter electrode used for loading samples was either Ni, or in the case where open cell potential measurements were made, NiOOH. The bath was covered by a lucite top to prevent evaporation of the water solvent, which otherwise would have changed the molarity

* Corresponding author. Tel.: +1-314-935-3762; fax: +1-314-935-6219. E-mail address: ehm@wuphys.wustl.edu (E.H. Majzoub).

of the solution. The reference electrode used for the open cell potential measurement was RHE. In the controlled loading experiment the solution was purged for 30 min with Ar while the whole cell was contained inside an Ar filled box.

When a sample was removed from the electrolytic cell, care was taken to separate and keep only pieces of sample that had been immersed in the KOH solution, and thus exposed to the hydrogen. The samples were washed with ethanol, ground to a powder and washed again, then heated to 30°C to evaporate any hydrates present. These samples were subsequently re-examined by X-ray diffraction and electron microscopy.

3. Hydrogenation

A comparison of the X-ray diffraction patterns in Fig. 1 shows a large shift to lower angle after hydrogenation. The change in low-angle peak positions by nearly 2° in 2θ corresponds to an expansion of the quasilattice of approximately 7%, consistent with an H/M value of 1.74 [3]. A comparison of these diffraction patterns with those hydrogenated by gas phase or ball milling shows that the crystalline hydride phase peak, often located on the low-angle side of the (100000) quasicrystal peak in hydrogenated samples, is greatly reduced in the electrolytically loaded samples [3].

The X-ray diffraction pattern from the hydrogenated 1/1 phase (W-phase) is contrasted with the pattern from the non-hydrogenated phase in Fig. 2. A small amount of undesired crystalline hydride is evidenced by the small peak (indicated by the vertical arrow) located at 33.4° in 2θ , below the (530) 1/1 peak. This precipitate is present in almost all of the 1/1 samples made. The separation of the (530) and (532) peaks in the hydrogenated sample (indicated by the horizontal arrow) is 1.94° in 2θ . This is larger than the separation of 1.84° between the corresponding (100000) and the (110000) peaks in the hydrogenated quasicrystal.

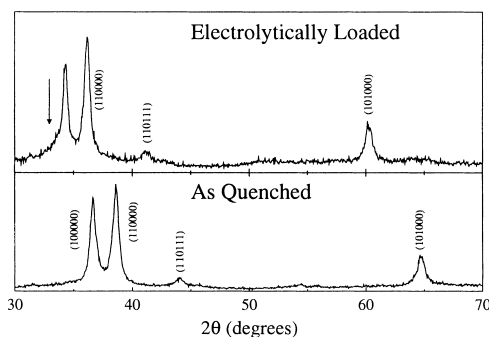


Fig. 1. X-ray diffraction patterns of as-quenched and hydrogenated quasicrystals. The quasicrystal peaks have been indexed following [2]. The arrow shows the position of the strongest peak from the crystalline hydride phase.

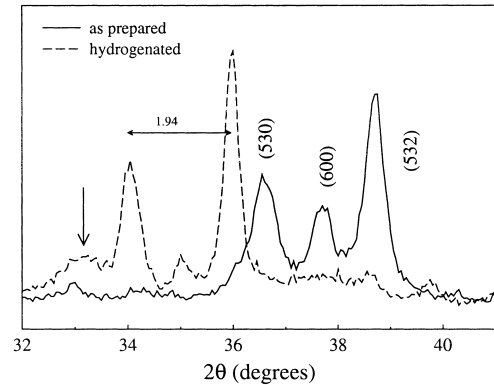


Fig. 2. X-ray diffraction patterns from as-cast and hydrogenated samples of the 1/1 crystal approximant phase (W-phase).

4. PC-isotherms from gas-phase loading

The vapor pressure of hydrogen in solution is a measure of the chemical potential of the hydrogen in the host metal. This is related to the local chemistry around the hydrogen interstitial site. The vapor pressure as a function of hydrogen concentration at constant temperature (PCT) was measured in rapidly quenched $Ti_{45}Zr_{38}Ni_{17}$ i-phase ribbons and in $Ti_{50}Zr_{35}Ni_{15}$ 1/1 approximant phase ingots, prepared as described above. Measurements were made between 300 and 400°C. To remove the oxide barrier, which inhibits hydrogenation, all samples were plasma etched and coated with a thin layer (≈ 20 nm) of Pd [4]. The Pd prevents further oxidation and aids the molecular hydrogen dissociation step.

Fig. 3 shows the equilibrium vapor pressure at 300°C for the i-phase and the 1/1 phase as a function of H/M . For both samples, the vapor pressure remains low ($< 10^2$ Pa) below $H/M \approx 1$, increasing sharply with increasing H/M above this value. For comparison, the measured vapor pressure at 350°C for a metallic glass of similar composition is also shown. A plateau of small slope in the vapor pres-

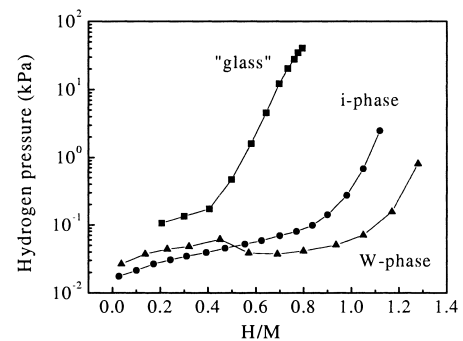


Fig. 3. The equilibrium vapor pressure at 300°C for hydrogen as a function of hydrogen concentration (H/M) for $Ti_{45}Zr_{38}Ni_{17}$ i-phase ribbons (solid circles) and $Ti_{50}Zr_{35}Ni_{15}$ 1/1-phase ingots (solid triangle). The vapor pressure for a $Ti_{45}Zr_{27}Ni_{20}Si_8$ "glass" is shown for comparison. The curves are provided as an aid to the eye.

sure curves is generally observed for simple crystal metal hydrides, reflecting ordered interstitial sites with a narrow energy distribution. In contrast, the vapor pressure curves for metallic glasses typically show no clear pressure plateau, reflecting a broad distribution of sites. The low initial slope, below $H/M = 0.3$, of the $\text{Ti}_{45}\text{Zr}_{27}\text{Ni}_{20}\text{Si}_8$ implies an additional narrow distribution of strongly binding sites and suggests that the material may be nanocrystalline rather than amorphous. The character of the vapor pressure curve for the quasicrystal is more like that of the 1/1 approximant, indicating a broad, weak plateau. While our measurements indicate that the plateau is stronger in the 1/1 phase, the vapor pressure often decreases in that phase with increasing H/M for intermediate levels of hydrogenation, Fig. 3. X-ray diffraction data indicate that this is due to the formation of a crystal hydride [5], which has a very low vapor pressure. The amount of hydrogen absorbed by the 1/1-phase ingots is $\approx 0.17H/M$ higher than the quasicrystal ribbons. While this may reflect small structural differences between the i-phase and 1/1 atomic structures, it more likely reflects the formation of the crystal hydride phase.

In principle, the site energy distribution for hydrogen in these phases can be computed from the vapor pressure data. A difference in the calculated distributions for the i-phase and the 1/1 phase was reported from our earlier vapor pressure measurements [6]. For both phases, a prominent peak was centered near -0.19 eV; a less prominent one was centered between -0.06 and -0.09 eV. The energy distribution of the prominent peak was narrower in the 1/1 phase, suggesting a more homogeneous site chemistry. Site energy distribution calculations, however, are strongly dependent on the local slope of the PCT curves. As shown, the formation of the crystal hydride phase can significantly influence this, making the conclusions drawn from our earlier work uncertain. Recently, we have shown that the introduction of a small amount of Pd (2–4 at.%) significantly decreases the crystal hydride formation. PCT measurements are currently being made on i-phase and 1/1-phase samples containing Pd to yield better estimates of the site energy distributions in these two structures.

5. Icosahedral glass model

While the icosahedral glass model suffers problems such as a 50% density deficit, accurate atomic models of quasicrystals are difficult to construct, and the icosahedral glass model accounts for some important structural features.

A constrained icosahedral glass was generated by Robertson and Moss [7] to model the Al–Mn–Si i-phase from its 1/1 approximant. We have made a similar calculation for the Ti–Zr–Ni i-phase based on its closely related approximant phase, the W(1/1), which consists of Bergman

icosahedral clusters packed face to face along the $\langle 111 \rangle$ directions of the cube [10,11]. A glass of bare sites was started with an icosahedral seed at the origin and grown by the addition of face packed icosahedra. New glass sites were defined at the centers of the joining icosahedra. The site-to-site distance between icosahedra was restricted, locally only, to a finite set corresponding to those found in a modified three-dimensional Penrose tiling [7]. A second constraint was imposed on the growing glass structure as each new icosahedron attempted to join existing sites. The glass grew, by attachment only, within a bounding sphere of fixed radius, until the number of unsuccessful attempts to place a new icosahedron reached a predetermined limit. The radius of the bounding sphere was then increased, allowing the model to continue to grow outward. These constraints increase the resulting cluster density to $\sim 88\%$ of that of a BCC packing. Our bare glass has a packing fraction of 0.60, which is comparable to a canonical cell packing [8]. In fact, it is known that such a tightly constrained icosahedral glass has a similar local environment as a canonical cell tiling [9]. The bare glass is decorated by non-distorted Bergman clusters, all placed with the same orientation, on each of the glass sites.

The Bergman clusters were decorated based on information obtained from neutron and X-ray diffraction studies of the 1/1 approximant, which has two-shell distorted icosahedral clusters sitting at the origin and body centers, and distorted third shells completing the inter-cluster “glue” [11]. The chemistry of the decoration is given in Table 1. The model has 540 000 atoms placed on 12 000 Bergman clusters. The resulting chemistry of the glass is $\text{Ti}_{26.7}\text{Zr}_{44.4}\text{Ni}_{28.9}$, with a density of 2.9 g/cm³, which is 48% of the experimental density of 6.06 g/cm³. This composition is very different from that of the quasicrystal and reflects that of the cluster only.

Simulated diffraction patterns were calculated by Fourier transforming and summing the pair correlation functions between each species. Instead of performing the pair correlation sums over all atoms in the model, which scales as N^2 , a Monte Carlo approach was used. The lattice points were sampled at random for 10^8 pairs for each correlation function. These functions were fit to a fifth order polynomial, which was subtracted, and the result was sine transformed according to $S_{AB}(k) = \int P'_{AB}(\sin kx/kx) dx$ for each value of k . The $S(k)$ were given the appropriate weights according to composition and then summed to give the final result.

Table 1
Bergman cluster decoration for minimum cluster separation of 124 Å

Site	Chemistry	Distance (Å)
Center	Ni	0.0
First-shell vertex	Ti	2.614
Second-shell vertex	Ni	5.228
Second-shell face	Zr	4.447

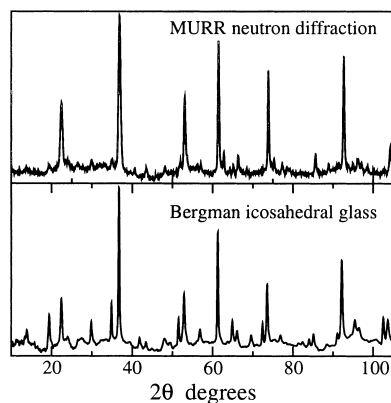


Fig. 4. Simulated diffraction of $\text{Ti}_{41.5}\text{Zr}_{41.5}\text{Ni}_{17}$ icosahedral phase with Bergman cluster icosahedral glass model.

The powder-averaged diffraction from this model is compared with the experimental data in Fig. 4. Although the glue sites are not present in this model, peak positions and relative intensities are well represented by the six most intense peaks in the real data. Small correlations in the glue are inferred from canonical cell tiling models [11]. A Rietveld refinement of the 1/1 phase shows that changes in the glue atom positions, however, result in only small changes in χ^2 in the range 1.2–1.4, indicating the diffraction is relatively insensitive to glue atoms due to their disorder. The increase in diffuse scattering in the simulation are due to the Zr and Ti pair correlation functions, which consist of second-shell face, and first-shell vertex positions, respectively. Similar diffuse scattering appears in the experimental data as well.

6. Conclusion

There is evidence for a fundamental cluster in Ti–Zr–Ni i-phase and its 1/1 approximant from diffraction studies. The electrolytic loading of hydrogen, and the preliminary vapor pressure data offer the possibility of obtaining new local structural information.

Acknowledgements

This research was partially supported by the NSF under grant No. DMR 97-05202.

References

- [1] X. Zhang, R.M. Stroud, J.L. Libbert, K.F. Kelton, *Phil. Mag. B* 70 (1994) 927.
- [2] P.A. Bancel, P.A. Heiney, P.W. Stephens, A.I. Goldman, P.M. Horn, *Phys. Rev. Lett.* 54 (1985) 2422.
- [3] A.M. Viano, E.H. Majzoub, R.M. Stroud, M.J. Kramer, S.T. Misture, P.C. Gibbons, K.F. Kelton, *Phil. Mag. A* 78 (1) (1998) 131.
- [4] J.Y. Kim, P.C. Gibbons, K.F. Kelton, *J. Alloys Compounds* 266 (1998) 311.
- [5] J.Y. Kim, P.C. Gibbons, K.F. Kelton, in preparation.
- [6] J.Y. Kim, E. Majzoub, P.C. Gibbons, K.F. Kelton, *MRS Symp. Proc. Quasicrystals* 553 (1999) 483.
- [7] J.L. Robertson, S.C. Moss, *Z. Phys. B* 83 (1991) 391.
- [8] C.L. Henley, *Phys. Rev. B* 43 (1991) 1.
- [9] M.E.J. Newman, C.L. Henley, *J. Non-Cryst. Solids* 153–154 (1993) 205.
- [10] W.J. Kim, P.C. Gibbons, K.F. Kelton, W.B. Yelon, *Phys. Rev. B* 58 (1998) 2578.
- [11] R.G. Hennig, E.H. Majzoub, A.E. Carlsson, K.F. Kelton, C.L. Henley, W.B. Yelon, S.T. Misture, *Mater. Sci. Eng. A* 294–296 (2000) 361–365.